ELSEVIER

Polymer 43 (2002) 2747–2760

polymer

www.elsevier.com/locate/polymer

Influence of cure via network structure on mechanical properties of a free-radical polymerizing thermoset

Manisha Ganglani[a,b], Stephen H. Carr[a,b], John M. Torkelson[a,b,*]

[a]*Department of Materials Science and Engineering, Northwestern University, Evanston, IL 60208-3120, USA*
[b]*Department of Chemical Engineering, Northwestern University, Evanston, IL 60208-3120, USA*

Received 29 August 2001; received in revised form 27 November 2001; accepted 29 November 2001

Abstract

An improved understanding has been achieved regarding the relationships among cure chemistry, network structure, and final physical properties of vinyl ester (VE) resins, a thermoset polymer often used as the matrix of fiber reinforced polymers. Mechanical properties of the polymer are found to depend on both cure schedule and cure formulation. The possibilities of phase separation and micro-gel formation being the cause for these differences in mechanical properties are examined. The VE/styrene (S) system does not phase separate under the conditions studied. Though bulk properties of the resin are unaffected by the details of the cure, the microscopic morphology, in particular the type of cross-link formed (intermolecular bond or intramolecular bond), is sensitive to both cure temperature and initiation mechanism as determined by cure formulation. An analysis of cure kinetics shows that both temperature and initiation mechanism affect the apparent 'reaction order' of the VE/S system as determined by the autocatalytic equation. This apparent reaction order is interpreted as being an indication of the degree of heterogeneity in the resin. By controlling cure temperature and cure formulation, it is possible to minimize the apparent reaction order and thereby optimize physical properties. Finally, a theory is adapted from other non-network polymer systems to qualitatively describe how cure temperature and initiation mechanism may alter the heterogeneity in network structure via micro-gel formation and how these changes in structure affect changes in the mechanical properties.

Keywords: Thermoset cure; Vinyl ester resin; Mechanical properties

1. Introduction

Vinyl ester (VE) resins are free-radical polymerizing thermosets used in fiber reinforced composites. Structurally similar to unsaturated polyesters (UPE), VE resins were developed to overcome the chemical resistance shortcomings of UPE resin. As a result of this relationship and because UPE resins have been studied in greater depth than VE resins, numerous characteristics of the UPE cure have been attributed to VE cure as well. In conventional polyester resins, the ester groups and carbon–carbon double bonds are located along the polymer chains, shown in Fig. 1, and are distributed randomly in the polymer network formed after co-polymerization and cross-linking with styrene. In VE resins, the ester units and carbon–carbon double bonds (forming methacrylate-type double bonds) are located only at the ends of the VE monomer.

The heterogeneity of free-radical cross-linking systems is an inherent result of the physical aspects of the free radical reaction and is often explained through micro-gel theory. Micro-gels are domains of high cross-link density dispersed in a pool of non-cross-linked material. The widely accepted concept of micro-gel formation describes structure build-up during cross-linking chain polymerization occurring at very low conversion, where a limited number of small, densely cross-linked clusters of high molar mass arise [1–10]. Cross-links then form between the clusters until macroscopic gelation occurs. During the rest of the reaction, the monomer is gradually incorporated into the growing network. High levels of intramolecular bonding characterize micro-gel formation. Although both intramolecular and intermolecular bonding result in cross-links, the latter leads to useful network cross-links while the former leads to unnecessary cyclization.

FTIR [1,2,7,10–15] and ESR [10] spectroscopy have shown that the conversion of UPE and VE unsaturations is higher than the conversion of styrene until substantial

* Corresponding author. Address: Department of Materials Science and Engineering, Northwestern University, Evanston, IL 60208-3120, USA. Tel.: +1-847-491-7449; fax: +1-847-491-3728.

E-mail addresses: manisha@northwestern.edu (M. Ganglani), s-carr@northwestern.edu (S.H. Carr), j-torkelson@northwestern.edu (J.M. Torkelson).

0032-3861/02/$ - see front matter
PII: S0032-3861(01)00805-9

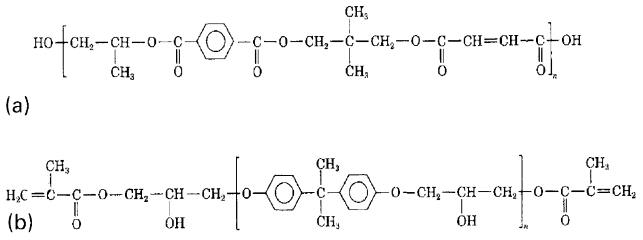

Fig. 1. (a) UPE oligomers. Unsaturations and ester groups are part of the repeat unit, resulting in multiple unsaturations and ester groups (hence the name polyester) along the chain. Because the reactive groups are within the repeat units, the number and placement may vary widely. (b) VE oligomer. Unsaturations and ester groups are outside the repeat unit, resulting in two unsaturations and esters for every molecule, regardless its size. Because the reactive groups are outside the repeat units, the reactive groups are only at the ends of the polymer chain.

overall conversion (much after gel), after which styrene consumption is greatly enhanced. Ganem et al. [15] and Ziaee and Palmese [1] have shown that about 40% of VE unsaturations are available when the reaction becomes limited essentially to styrene monomers only, which has led some to conclude that the remainder of the reaction is due to styrene homopolymerization.

The observation of increased styrene (S) reactivity near cure completion has led researchers to associate the formation of micro-gels with the occurrence of polymerization induced phase separation (PIPS) in both UPE/S and VE/S systems. In PIPS, polymerization and phase separation occur simultaneously. Numerous systems are thought to undergo PIPS: non-cross-linking systems that are based on free radical polymerization [16–19]; cross-linking systems such as rubber-modified epoxy systems based on DGEBA [17,20–22]; and thermoplastic-modified thermoset systems [17,23,24]. Proof of phase separation comes from light scattering experiments [17,21,22]. In cross-linking systems, it has been noted that phase separation occurs in the pre-gel state [13,20,25]. Micro-gel formation in step-polymerizing epoxy systems has been proven to be associated with phase separation [26]. However, Boots [27] showed that micro-gel formation is an inherent consequence of chain reactions, regardless of the presence or absence of phase separation. (Micro-gel formation may be distinguished from phase separation in the following manner. If the micro-gel formation is not accompanied or preceded by a thermodynamically driven process or if the composition of the resulting micro-gels is similar to that of the other material in the system, the system is not considered to be phase separated but rather consists of 'sol' and 'gel' fractions, the latter of which are confined to small, discrete regions within the system.)

In vinyl–divinyl systems, though evidence points to phase separation at molar ratios (vinyl to divinyl) of 4 or higher [1,10], direct evidence points to the lack of phase separation in VE systems having the optimum molar ratio of 2 [10,13]. Further, polystyrene cannot be extracted from the fully cured VE resin, which shows that each individual polystyrene chain is either well entangled within the matrix or that each chain is independently grafted to the matrix [28]. Dynamic mechanical analysis studies also show an alpha-relaxation at 120 °C but clearly not at 100 °C, the latter expected if polystyrene is formed and develops its own phase. These results point to miscibility of VE/S co-polymer and polystyrene that may form during VE resin cure [29].

Recently, more concrete experimental evidence has been presented that indicates that micro-gel formation does not need to be associated with phase separation. Gel permeation chromatography results show shrinkage of the UPE micro-gels at early stages of the curing reaction [30]. This could result from a polymer intramolecular cyclization process in which many pendant polyester vinyls may be trapped in compact micro-gels, retarding effective vinyls from further intermolecular reactions. Nanometer-sized particles have been isolated and found to be densely cross-linked with conversions of 60–70%. The presence of trapped radicals early in the reaction has pointed to the presence of regions of high cross-link density/low mobility while the bulk of the system is still in the liquid or rubbery state [3]. The observations of low mobility and high cross-link density suggest that the clusters undergo not only micro-gelation [31,32] but also micro-vitrification when the cure temperature is below the ultimate glass transition temperature, T_g. Observations of the patterns of viscosity change with conversion also support this theory [33,34] as do comparisons of results from dynamic mechanical analysis and measurement of charge-recombination luminescence on acrylate resins [35].

In vinyl–divinyl co-polymer systems such as UPE/S or VE/S, the focus of much research has been on understanding the effect of monomer composition ratio on micro-gel morphology [2,28], but relatively little work has been done to analyze the effect of initiation mechanism on the cure kinetics of a VE resin [36]. Further, though much work has gone into the study of cure chemistry, little has been done to determine its relationship with the physical properties of VE/S thermosets. The present study attempts to narrow this gap in understanding by investigating the relationship between cure chemistry (in particular, radical concentration and system mobility), network structure, and physical properties of VE/S resins as a function of initiation mechanism.

Cure of the VE/S resin involves initiator and, as an option, accelerator. At high temperatures and in the absence of accelerator, thermal reaction of initiator is responsible for the production of free radicals. However, the use of accelerator in VE/S polymerizations has significant consequences [37–39]. The chemistry of the initiation is quite complex, but in the simplest terms, the initiator is the active element and the accelerator, having no direct effect on the resin system, catalyzes the initiation process. The initiator/accelerator system used in this research is benzoyl peroxide (BPO)/*N*,*N*-dimethylaniline (DMA). The acceleration of the BPO by the DMA is considerable at 10^6-fold for a 0.01 M

Table 1
Cure formulations employed in this research

Ingredient	Formulation 1 (parts by weight)	Formulation 2 (parts by weight)	Formulation 3 (parts by weight)
DERAKANE 411-350	100	100	100
BPO	1	1	1
DMA (10% in styrene)	0	0.1	0.2

DMA solution [37]. Thus, whereas the release of radicals during thermal initiation is a slow and steady process, accelerated cures lead to the immediate introduction of radicals. Therefore, it is expected that the presence of the accelerator will have a significant impact on the network structure of the resin.

2. Experimental

DERAKANE® 411-350, a Dow Chemical VE resin containing 45 wt% styrene, was used as purchased without the removal of inhibitors present in the resin. The initiating system was comprised of 75% active benzoyl peroxide in powder form and 99% purity *N*,*N*-dimethylanaline, both from Aldrich. The formulations tested are given in Table 1. The BPO was first dissolved in styrene on a 1:1 weight basis. The appropriate amounts of BPO/S solution and 500 g of DERAKANE® were poured into a plastic bottle that was vigorously shaken to achieve optimal mixing. The bulk mixture was stored at 4 °C to prevent premature reaction. The DMA was kept separately in a 10 wt% styrene solution at 4 °C. Immediately prior to each experiment, the appropriate amounts of DMA and resin solution were stirred together. The cure schedules for the mixtures are shown in Table 2. It must be noted that although these schedules indicate isothermal cures, reaction runaway often leads to actual cure temperatures greater than those intended. The one exception would be resins cured in the differential scanning calorimetry (DSC) where isothermal cure temperatures are closely monitored and maintained.

For both tensile and fracture toughness tests, aluminum molds for making specimens via the cure schedules in Table 2 were designed using Pro-Engineering software and created using a computer numeric control (CNC) machining center. A 1.5% draft was incorporated in the designs to ease the release of the molded sample. An epoxy mold release was sprayed prior to filling of the mold for the same purpose. Samples were end-milled to remove all visible defects on the relevant surfaces. Tests were carried out using a computer-controlled Sintech 20/G screw-driven universal test frame. Tensile bars were of Type M-1 (ASTM standard 638 M). The samples, carefully aligned parallel to the grips, were pulled at a rate of 5 mm min^{-1}. The extensometer attached to the tensile bars and the Sintech were both calibrated prior to use. Toughness tests were carried out in accordance with ASTM standard D-5045. A pre-cracked single-edge notch-bend specimen for three-point bend tests was used. The crosshead speed was set at 0.05 in./min. The Sintech was calibrated prior to use.

Table 2
Cure schedules employed in this research

Cure		Post-cure	
Temperature (°C)	Time (h)	Temperature (°C)	Time (h)
30	15	135	2
60	2	135	2
90	2	135	2

Each of the three formulations of the resin was individually tested for phase separation at each of the three temperatures. Mixtures were prepared, smeared across a microscope slide with a wooden stick, and then covered with a coverslip. Samples were kept on ice for the short time between preparation and experimentation to prevent reaction prior to data collection. Samples were viewed using a Nikon transmission light microscope outfitted with a hot stage. A Colorado Video, Inc. Model 310 A Video Integrator was attached to both the microscope and a multimeter. Once the hot stage reached the desired temperature, the sample was placed on the hot stage and the temperature maintained. The voltage was read periodically throughout the duration of cure. SAXS measurements were done on an instrument having a sample to detector-slit distance of 375 mm and a 100 μm source size rotating anode. Nickel-filtered Cu Kα radiation ($\lambda = 0.154$ nm) was employed, measured with a scintillation counter and a pulse-height analyzer. The scattering angle range was $0.022 < 2\theta < 5.3°$. Sample collections ranged from 4 to 12 h.

Network characterization was done by measuring density and swelling in solvent. Distilled water was mixed with NaCl (14–19%) to create 150 ml salt water solutions having distinct densities [40]. Samples were parts of post-cured tensile specimens or fracture toughness specimens that had already been molded, milled, and tested. Three measurements were conducted for each sample in each solution. Samples were individually immersed in each NaCl solution and left for 2 min to reach equilibrium. An observation of sink/float was recorded for each sample in each solution. Prior to these density tests, samples had been tested for water absorption, revealing no swelling in water over a three-week period. Samples used for both density and swelling tests were broken from the post-cured tensile specimens, and swelling experiments were carried out at room temperature with acetone as the swelling agent.

For FTIR experiments, thin films of each of the nine

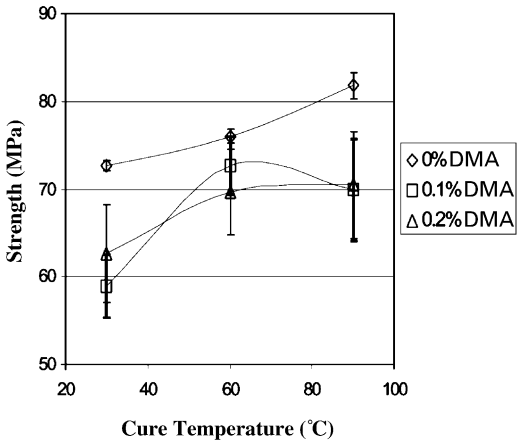

Fig. 2. UTS after post-cure versus cure temperature for samples with varying accelerator concentration. UTS depends on both cure temperature and formulation. Higher tensile properties are associated with thermally initiated samples and higher cure temperatures. As a reference value, the tensile strength of polystyrene is 46.2 MPa. Error bars represent one standard deviation.

samples were cured between two Teflon sheets and pressure was applied with weighted clamps. Three sets of each film were made independently to minimize error. Spectra were acquired using BIORAD FTS-60 FTIR spectrometer purged with air cleaned of water and carbon dioxide gas. Sixty scans were taken over a wavenumber range or 400–4000 cm^{-1} at a resolution of 2 cm^{-1}. Band area and position measurements were obtained using standard WIN-IR software. The baseline was subtracted from the final spectra and a ratio of peaks then taken. The peak at 912 cm^{-1} represents styrene unsaturations while the peak at 945 cm^{-1} represents VE unsaturations. The relative differences in VE/S unsaturations can be characterized by taking a ratio of these peak heights.

DSC measurements included both isothermal and temperature scans. Samples of 10–30 mg of each of the three formulations were individually sealed in a stainless steel pan. To minimize the reaction prior to measurement, the samples were kept in a methanol/dry ice slurry until ready for testing. The experiment was carried out with a Perkin–Elmer DSC 7 under nitrogen gas using ice water to maintain temperature. For temperature scan tests, samples were heated from 25 to 250 °C at a rate of 5 °C min^{-1}. A second temperature scan was also performed to identify T_g. For isothermal scans, each formulation was tested at each of the three cure temperatures (30, 60, 90 °C) until the reaction reached completion. A temperature scan from 25 to 250 °C at a rate of 5 °C min^{-1} was then conducted to complete the reaction. A second temperature scan was taken to obtain T_g.

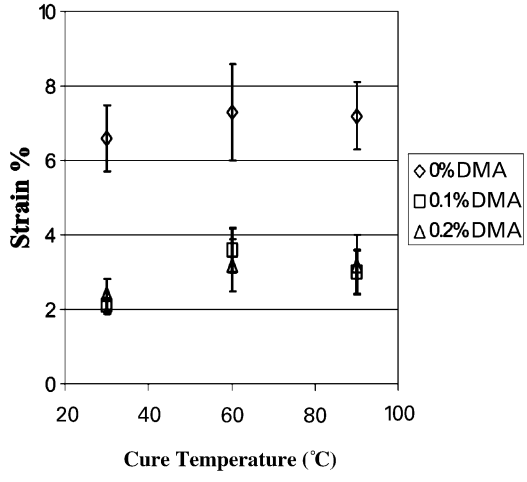

Fig. 3. Strain-at-break results for all samples verses cure temperature for all resin formulations. The dependence of results on the presence/absence of accelerator during cure is much stronger than the temperature dependence of the results. Error bars represent one standard deviation.

3. Results and discussion

3.1. Mechanical and physical properties

Several trends reveal that the presence or absence of accelerator during cure as well as the cure temperature have significant impact on tensile properties of the cured resin. First, when cured with accelerator, the samples break shortly after yield, or the onset of plastic deformation. When thermally initiated (no DMA), the samples fracture in a more ductile manner, displaying a maximum in the tensile strength before fracture. Second, employing DMA for the cure or curing at lower temperatures reduces the ultimate tensile strength (UTS), also shown in Fig. 2. For any of the three cure temperatures examined, the thermally initiated sample has the greatest UTS. Third, the variability of the UTS results increases for accelerated samples as compared to thermally initiated samples. The increasing standard deviation with increasing accelerator concentration reveals lower reproducibility of results. From this, one may infer greater variability of the structure. Fourth, employing DMA reduces the strain-at-break values, also shown in Fig. 3. The results are much more dependent on the mode of initiation than the temperature of cure. Regardless of the cure temperature, accelerated initiation results in maximum strain values between 2 and 4% whereas with thermal initiation, the strain doubles to values between 6 and 8%. Though UTS showed a dependence on both initiation mechanism and cure temperature, strain-at-break shows a much stronger dependence on initiation mechanism.

In contrast, the shape of the stress–strain curves is identical until yield, leading to a nearly constant value for Young's modulus (3.3 GPa). This indicates that changes in cure schedule and formulation do not alter the material composition.

It has been shown that the conversion of terminal methacrylates in the VE/S system reaches a maximum at 45 wt% styrene [15]. At this styrene concentration, it has also been found that tensile strength and elongation [29] reach

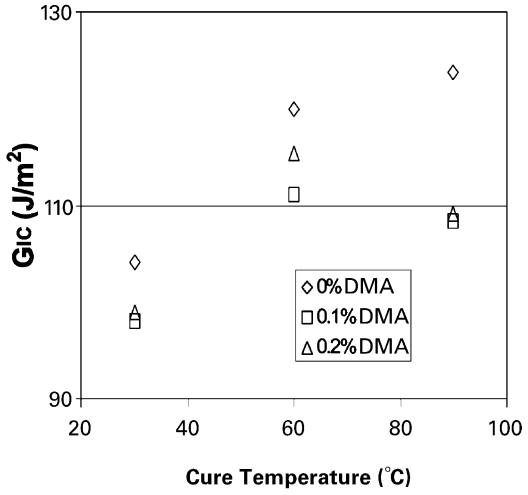

Fig. 4. Strain energy release rate results versus cure temperature for all resin formulations. Samples cured without accelerator have higher strain energy release rate values at all cure temperatures. Further, G_{IC} increases with cure temperature except for the accelerated 90 °C cure resin.

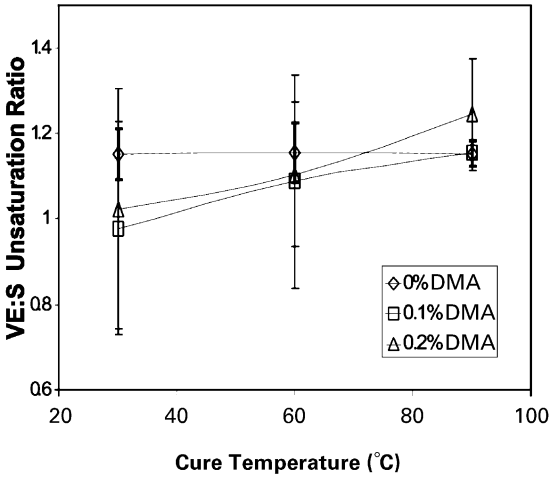

Fig. 5. Dependence of VE: styrene unsaturation ratio on cure temperature. Results are for post-cured samples.

maximum values. Thus, it may be inferred that maximum methacrylate conversion relates to greatest strength and elongation. Based on this statement, the results obtained previously suggest that high temperature cure without DMA, having the highest UTS and strain-at-break values, results in maximum methacrylate conversion.

Strain energy release rate (G_{IC}) data energy data may also provide insight on the network structure of the thermoset polymers. In order to create new surfaces in a thermoset, numerous chemical bonds must be broken. A network with greater intermolecular cross-links will require the rupture of many more bonds, and therefore require more energy. Fig. 4 shows the G_{IC} data for each of the samples. The trends observed for the strain energy release rate are also similar to those for the tensile results. For the thermally initiated samples, those cured at higher temperatures require greater energy for fracture. When accelerator is used, the cured samples require less energy to create the fracture surfaces at each cure temperature. Further, the peak in properties for accelerated resins is observed for the 60 °C cure, indicating that accelerated resins form the most 'effective' network when cured at 60 °C.

Fracture surfaces of the toughness-test samples were also examined via SEM. Although none of the fracture techniques resulted in an observation of nodular morphology throughout the entire fracture surface, some techniques yielded regional pockets that resembled nodular features. In addition, the sample cured with DMA displayed greater texture at the fracture surface whereas the thermally initiated sample is more featureless. For specimens without pre-cracks, Kausch [41] found that excess elastic energy is stored in the sample at the moment of rupture. This excess energy is expended in the creation of increased fracture surface area giving rise to rough surfaces. The SEM results indicate that greater elastic energy is stored in the samples made with DMA, which could be the result of increased stress within the system.

The phase separation (light transmission and SAXS) studies, which should provide information on the presence of phase separated structures with dimensions on the order of 100 nm or greater (via light transmission) and 0.1–60 nm (via SAXS), yielded null results. Regardless of cure temperature or accelerator concentration, no change in light transmission and no peak development in SAXS occurred throughout the cure. These results argue against the interpretation of previous FTIR studies [1] that the dominating styrene–styrene reaction at high cure levels is an indication of phase separation or the formation of a polystyrene matrix or that micro-gel structures are located within a polystyrene matrix.

Likewise, the density and swelling studies revealed no significant difference in the systems as a function of cure temperature and accelerator concentration. The density was $\sim$1.133 g cm^{-3} for all post-cured samples, regardless of cure history. The swelling results showed a relatively consistent equilibrium uptake of solvent (38% by weight) and suggest that many of the connections between cross-links are short, possibly occupied by as little as one or two styrene units, and/or that there exist numerous dangling ends off of the network structure.

3.2. FTIR and DSC analysis

Fig. 5 summarizes the results of the FTIR analysis of the post-cured resins. The VE/S unsaturation ratio is defined as the number of unsaturations belonging to the VE molecule divided by the number of unsaturations belonging to styrene monomers. The VE/S ratio prior to any reaction is 0.28, meaning that for each VE unsaturation there exist 3.6 styrene unsaturations. This ratio changes throughout the reaction as vinyl and vinylene groups are consumed, and the final ratio is dependent on cure conditions. A decrease

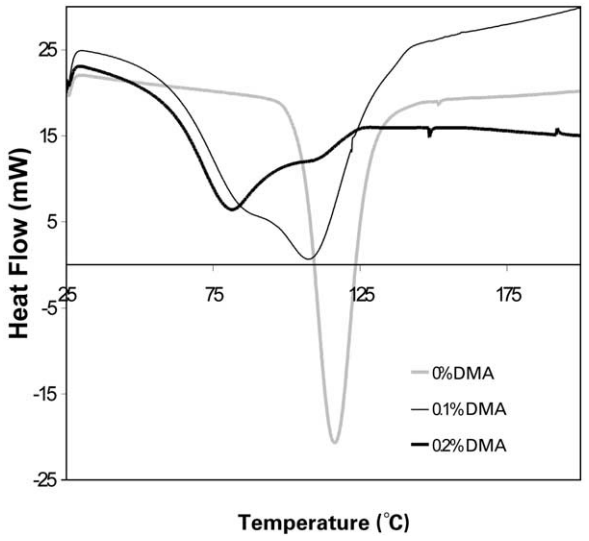

Fig. 6. DSC temperature scans based on accelerator concentration. Without accelerator, only one exotherm peak at 115 °C is evident. When accelerator is added, a second peak arises at 80 °C. The second peak becomes proportionately larger with increasing accelerator concentrations.

in the ratio indicates that either more VE unsaturations have reacted or numerous styrene unsaturations (i.e. monomers) remain. Only trace amounts of styrene monomer remain after the post-cure, so increases in the ratio are more likely to represent unreacted VE monomer or dangling ends.

Although all post-cured, thermally initiated samples have a VE/S unsaturation ratio of 1.15 with low standard deviation; when DMA is employed, the lower the isothermal cure temperature, the lower the VE/S unsaturation ratio after post-cure. This indicates that lower cure temperatures are more conducive for the consumption VE unsaturations. In addition, the standard deviation of the VE/S unsaturation ratio is much higher for samples made with accelerator, attesting to greater sample heterogeneity.

Initially, it would appear that a lower VE/S ratio would indicate greater cross-linking, and this would have a positive outcome for the mechanical properties of the resin. However, the samples having the lowest VE/S ratio are those cured with accelerator at low temperatures, and these are the samples having the poorest mechanical properties. From these data, one may infer that although many more VE unsaturations lead to cross-links, these additional cross-links do not contribute to mechanical strength and hence must be 'wasted' in cyclization reactions.

Fig. 6 shows DSC temperature-scans during reaction of the resin with different DMA concentrations. Because all samples are subjected to the same thermal treatment, these results reflect only differences in cure due to different initiation mechanisms. Without accelerator, a single symmetric peak is seen at ~115 °C. When DMA is employed, the reaction begins at much lower temperature as expected, the exotherm peak broadens, and an additional peak arises at a lower temperature of ~80 °C. As the concentration of DMA is increased from 0.1 to 0.2%, the peak at ~80 °C becomes the larger, primary peak and that at ~115 °C is a smaller, secondary peak.

Table 3
Changes in enthalpy and T_g based on accelerator concentration

DMA (%)	ΔH (J g^{-1})	T_g (°C)
0.0	355 ± 28	114 ± 1.5
0.1	300 ± 87	112 ± 3.5
0.2	249 ± 91	107 ± 2.4

The observation of two exotherm peaks that vary in size and position indicates that the polymerization kinetics are complicated and suggests the occurrence of two reaction processes. The second exotherm peak has been taken to indicate styrene homopolymerization [14], consistent with indications of styrene homopolymerization from FTIR results [1,7,10,13–15]. Based on this theory, these data would indicate that a substantial population of polystyrene is established early in the conversion process, and mechanical tests and phase separation results do not support this hypothesis. The two peaks have also been attributed to unique initiation mechanisms: the first, initiation by accelerator, and the second, thermal decomposition of initiator [42,43]. However, given the 10^6-fold increase in radical concentration based on the presence of DMA, when accelerator is used, the mechanism for accelerated initiation would dominate strongly over the mechanism for thermal initiation, even at high cure temperatures.

Cook [44] hypothesized that the changes may be due to complex variations in k_p and k_t, the propagation and termination rate parameters. This explanation is plausible. With accelerator, the reaction begins at very low temperatures. However, after a certain extent of reaction, many radicals become trapped in 'cages' [3,10]. As the temperature increases, these radicals acquire the energy to escape from their cages and begin co-polymerization. Thus, the two peaks could indicate different times at which radicals were introduced into the system. A consequence of radical trapping would be that the first peak was indicative of intramolecular cross-link formation and the second peak of intermolecular cross-links, as proposed by Huang and coworkers [45,46].

Table 3 shows the change in enthalpy (ΔH) associated with reaction for temperature scans and the resulting reacted resin T_g for each resin formulation. With greater DMA, lower ΔH and T_g values are observed. The decrease in enthalpy at high accelerator levels indicates that fewer reactions occur with higher accelerator concentrations under non-isothermal conditions. When cross-linking and co-polymerization occur simultaneously, the effect of each on T_g must be considered independently. Cross-linking increases T_g and is largely independent of the co-polymerizing unit [47]. In the case of the VE/S system, the co-polymer effect (addition of styrene) lowers T_g. Because the styrene concentration in the resin is not altered among the formulations, the decrease in T_g with increasing

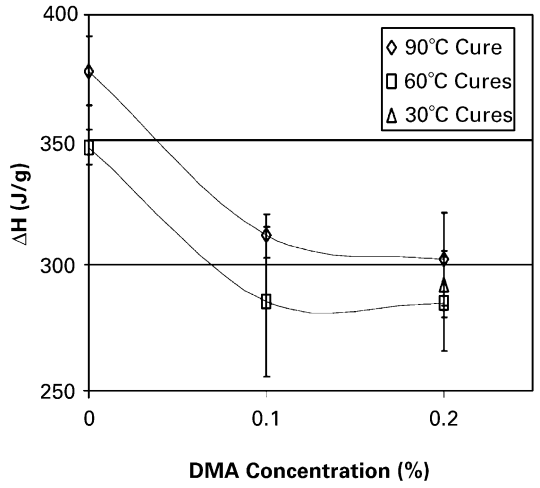

Fig. 7. The total change in enthalpy (including the post-cure reaction) during isothermal cure as a function of both accelerator concentration and cure temperature. The initiation mechanism has the greatest impact on the change in enthalpy. For accelerated samples, cure temperature appears to be more significant that the actual concentration of accelerator.

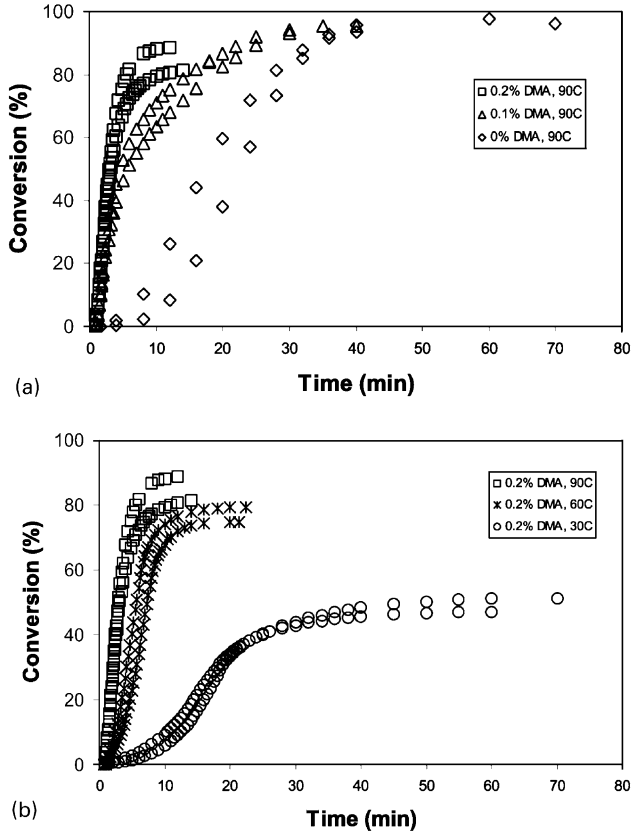

Fig. 8. (a) Isothermal scans for showing the effect of initiation mechanism on samples cured at 90 °C. Total conversion is based on reaction during isothermal cure and post-cure. Samples cured without accelerator achieve the highest conversions. (b) Isothermal scans for showing the effect of cure temperature on conversion for highly accelerated samples. Total conversion is based on reaction during isothermal cure and post-cure. Cure temperature is very significant in determining final conversion during isothermal cure in the lower temperature range of 30–60 °C.

accelerator may be explained by the cross-linking effect, which dictates that fewer cross-links form with increasing DMA concentration.

Fig. 7 shows the changes in enthalpy based on isothermal cures for samples subjected to a 135 °C post-cure after the isothermal cure. Unlike the dynamic temperature scan results, the data reveal that the number of reactions that occur is primarily a function of initiation method (accelerated or thermal) and cure temperature, but not the accelerator concentration. When accelerator is employed during isothermal cure, T_g decreases with increasing cure temperature, ranging from 112 °C for 30 °C cures (plus post-cure) to 100 °C for 90 °C cures (plus post-cure). Thus, higher isothermal cure temperatures prior to post-cure reduce the ultimate T_g for accelerated cures. The combination of the T_g and enthalpy data indicates that samples have varying T_g values even though the extent of reaction is similar. If the isothermal cure reactions were associated with the cross-linking effect, then enthalpy would be expected to increase with increasing T_g. Because this is not the case, changes in the glass transition based on changes in isothermal cure temperature and cure formulation cannot be attributed to the cross-linking effect.

Another explanation for the increased T_g at lower cure temperatures takes a more molecular point of view and states that the size of the cooperative motion critically depends on the amount of configurational entropy available [48]. The argument is made that it is the distribution of free volume that is responsible for the variations in T_g, where samples having greater heterogeneity have greater configurational entropy and therefore higher T_g. This theory suggests that accelerated samples isothermally cured at low temperature have greater configurational entropy and therefore greater heterogeneity that may be caused by large variations of intramolecular and intermolecular bonding.

Fig. 8 shows the effects of accelerator concentration and cure temperature on reaction rate during isothermal cure based on a total conversion that includes post-cure. Hence, the total conversion values used to develop these curves are larger for the thermally initiated samples than accelerated samples. The results reveal that reaction rate depends on both DMA concentration and cure temperature. The highest conversion during isothermal cure at 90 °C is achieved for thermally initiated samples and decreases progressively with greater accelerator concentrations. For accelerated samples (only the 0.2% DMA results are shown), maximum conversion increases with increasing cure temperature for the range studied. However, the change in conversion with increasing cure temperature is not gradual. The most significant change comes with the 30 °C and 60 °C cures. The conversion rates for 60 and 90 °C cures are very similar.

The cessation of polymerization prior to total monomer conversion has been widely observed in the cure of glass forming networks and, in the case of free-radical polymerization reactions, is often attributed to diffusional control

of the curing process which becomes important when T_g approaches very closely to the cure temperature [44,49,50]. Note that the level of conversion reached during isothermal cure is related to the mechanical properties of the resin. For example, thermally initiated samples reach the highest conversion during isothermal cure at 90 °C and have the best mechanical properties whereas the 30 °C cure of 0.2% DMA has the lowest conversion during isothermal cure and also the poorest mechanical properties. This indicates that a majority of the effective cross-links that provide the resin with its mechanical strength form during the isothermal cure, not during the post-cure.

3.3. Kinetics

In addition polymerization, the conversion of a double bond to a single bond is typically accompanied by an exothermic heat of reaction. The degree of cure or conversion α, may be defined by the ratio of the heat of reaction, Q_t, to the total heat of reaction, Q_T, equal to $Q_I + Q_R$ where Q_I is the total heat of reaction at the isothermal cure temperature and Q_R is the residual heat of reaction obtained upon a post-cure temperature ramp:

$$\alpha = \frac{Q_t}{Q_T} = \frac{Q_t}{Q_I + Q_R}$$

The rate of cure, $d\alpha/dt$ is then obtained by differentiating α with respect to time and is related to the rate of heat generated dQ/dt :

$$\frac{d\alpha}{dt} = \frac{1}{Q_T}\left(\frac{dQ}{dt}\right)_T$$

(It should be noted that the heats of reaction for styrene and methacrylate-based monomers are not identical on a per carbon–carbon double bond reaction basis. Thus, the definition of α employed here averages over the heats of reactions for the two types of carbon–carbon double bonds undergoing reaction in the specific VE/S system under study.)

Kinetic models relate species composition with time and temperature during a chemical reaction in the form of a reaction rate expression [51]. Some of these models are mechanistic while others are empirically based. Given that a complete understanding is still being sought [52–55] for the mechanistic kinetic model for the relatively simple cases of free radical polymerization of homopolymers made from methyl methacrylate and from styrene, both of which exhibit autoacceleration at moderate to high conversion, a mechanistic kinetic model will not be attempted for the much more complicated cross-linking, free radical copolymerization reaction being studied here. Instead, the autocatalytic equation, employed as an empirical equation, will be used to characterize curing kinetics of the thermosetting resin investigated here.

Kamal and Sourour [56] developed the autocatalytic equation for the curing reaction of thermosetting resins that correlates isothermal cure data with temperature and time by the equation, where k_1 and k_2 are temperature-dependent rate parameters, m and n are constants independent of temperature, and α is the relative degree of reaction.

$$\dot{\alpha} = \frac{d\alpha}{dt} = (k_1 + k_2\alpha^m)(1 - \alpha)^n$$

They conducted the isothermal tests where thermal initiation was the only method of initiation. The model yielded results that were in qualitative and quantitative agreement with typical experimental rate of cure and integral heat of cure data. Kamal and Sourour found $m = 0.25$ and $n = 1.75$, independent of temperature, for the system they studied. Calculated and experimental isothermal cure results for step growth polymerizations, epoxy systems in particular, have also shown excellent agreement between the autocatalytic model and experiment [57–61].

Several methods for solving for the autocatalytic variables exist. Ryan and Dutta [62] proposed a rapid estimation technique for the determination of the kinetic parameters k_2, m and n of the autocatalytic equation that describes epoxy cure based on parameters readily determined at any given temperature using DSC. Though the results are based on epoxy cure, Ryan and Dutta stated that the technique "may be applied successfully to any reaction that can be approximated" by the autocatalytic equation. Researchers [33,34,43,57,61] have validated the Ryan–Dutta method and given this rapid-estimation technique widespread credibility. Though Kamal and Sourour never defined the variables m and n as reaction orders or the sum $m + n$ as the overall reaction order, this assumption made by Ryan and Dutta had a significant impact. This second-order assumption has been applied to numerous thermoset systems, with or without validation.

The autocatalytic model has also been used in the VE system, usually under conditions of thermal initiation [63]. However, Lem and Han [33,34,43] studied both UPE/S and VE/S resins using the BPO/DMA initiating system. Making a second-order reaction assumption, they used the procedure suggested by Ryan and Dutta to calculate the values of m, n, k_1, and k_2 and found that accelerated cures for UPE/S and VE/S resins at temperatures of 40–60 °C show poor fits with the model based on the Ryan–Dutta method, especially after the reaction peak. They did not discuss the reasons for the poor fits. Similar results were obtained in this research (see Fig. 9). Better fits between experiment and model are found with samples cured at higher temperatures, in particular for the system that lacks accelerator. The fit worsens as the temperature is lowered. For samples cured isothermally at 30 °C, the model fits only at the peak point of the experimental data, overestimating the conversion rate both before and after the maximum. Hence, the autocatalytic equation, as solved by the Ryan–Dutta technique, is more effective with resins having fewer complexities (i.e. no accelerator or mobility restrictions).

The shape of the conversion rate curve is highly dependent on the cure temperature while its magnitude is highly

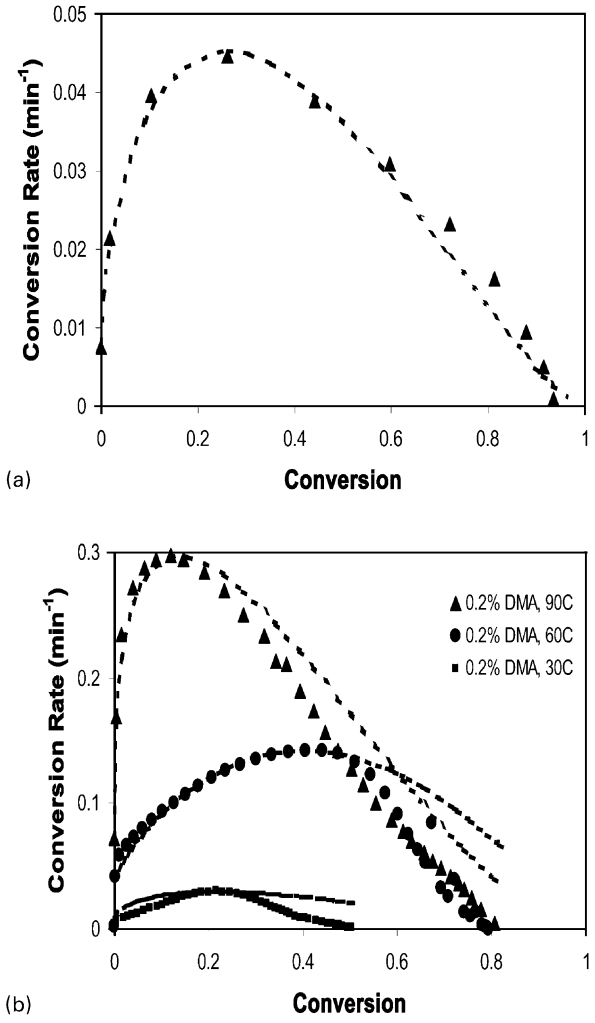

Fig. 9. (a) Cure at 90 °C without accelerator. (b) Cure at 30, 60, and 90 °C with 0.2% DMA.

dependent on accelerator concentration. At high cure temperatures of 90 °C, there exists a sharp initial rise in conversion rate that peaks at approximately 20% conversion. The magnitude of this rise increases significantly as accelerator concentration increases. This indicates that the radicals generated have trouble terminating at the onset of the reaction and that the radical population increases intensely with increasing DMA concentration. Numerous researchers [58,59,61,64] have employed such plots for UPE and VE systems cured with initiator but lacking accelerator and found that for cures at temperatures of ~90 °C, peak conversion rate does not exceed 0.07 min^{-1}. However, these results show that accelerated cures at the same cure temperature have significantly greater peak conversion rates of up to 0.4 min^{-1}.

The conversion rate falls rapidly after the peak. This overestimation of data by the model is a problem often encountered when trying to model thermoset systems. The higher reaction rate prediction of the model has been attributed the to the fact that the diffusion of the reactants and the dependence of the rate constants on the extent of cure were not accounted for in the model [65]. These two factors result in the fast decay of the reaction rate whereas the model assumes a finite value. In a free-radical polymerization, other factors such as initiator efficiency and cage effects may be responsible for the deviation. Wen and McCormick [66] studied the photopolymerization of dimethacrylates and also found that their mechanistic kinetic model overestimated the experimental data beyond the peak conversion rate. By adjusting their model to account for radical trapping, much improved fits were obtained.

At lower cure temperature, the change in conversion rate becomes more gradual. This does not indicate that the accelerator is less effective in generating radicals. Rather, because viscosity is higher at lower temperatures, radical mobility decreases at these lower temperatures resulting in cage return or lower initiator efficiency. Therefore, though an approximately equal number of radicals form at all temperatures for the 0.2% DMA cure, greater mobility at the higher cure temperatures allows for the radicals to escape quickly from their solvent cages and begin initiating numerous reactions. Early in the reaction, the high mobility allows for more propagation events than termination events resulting in a sharp spike in the conversion rate. At lower cure temperatures, limited mobility of the radicals moderates their release from the solvent cages and the number of propagation reactions that occur, resulting in lower conversion rates.

An alternative solution for modeling the experimental data is to remove the restriction of $m + n = 2$. Given that the autocatalytic equation is empirically rather than mechanistically based for the systems under study here, there is no implication of the sum of $m + n$ being related to a reaction order, and thus needing to be restricted in value. With the value of $m + n$ being allowed to float, the model was fit to the experimental data by a non-linear regression technique. Table 4 lists the values of k_s, m, and n resulting from the calculations, and Fig. 10 shows the resulting curves based on the autocatalytic model plotted against the experimental data. A much better fit with the experimental data throughout the entire extent of reaction is found.

The main distinguishing feature between the two methods of solving for the autocatalytic equation parameters is the absence of a second order reaction constraint for the non-linear regression technique. As a result, the apparent reaction order ($m + n$) can take on a wide range of values, as shown in Fig. 11. All 30, 60, and 90 °C data points are averages for at least three independent calculations. The apparent reaction order decreases with increasing temperature for samples employing accelerator but is nearly independent of DMA concentration.

Others who have attempted to model thermoset systems such as UPE [56,64], epoxy [61], or dicyanate [59], without

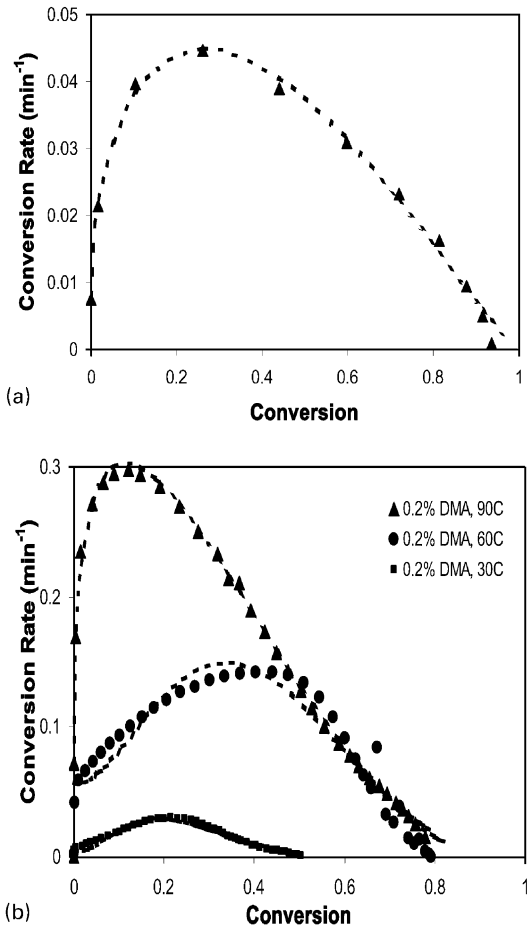

Fig. 10. (a) Cure at 90 °C without accelerator. (b) Cure at 30, 60, and 90 °C with 0.2% DMA.

a restriction on reaction order and using phenomenological techniques have found that the overall reaction order remains at reasonable levels of approximately two. However, they studied systems that involved thermal initiation at high cure temperatures where system mobility remained high. Under related conditions (0% DMA, 90 °C cure), similar results were observed in this research irrespective of the technique used to solve for the parameters. When the phenomenological approach lacking any mathematical restrictions is taken to describe an accelerated system, significant deviations in the results were obtained.

Table 4
Linear regression results: total heat of reaction

Sample	k_2 (min^{-1})	m	n	$m+n$
0/90	0.13 ± 0.02	0.53 ± 0.06	1.38 ± 0.16	1.84 ± 0.22
1/90	0.42 ± 0.23	0.40 ± 0.12	2.39 ± 0.44	2.79 ± 0.53
2/90	1.00 ± 0.27	0.55 ± 0.17	2.24 ± 0.36	2.79 ± 0.53
1/60	2.31 ± 0.81	1.80 ± 0.19	3.99 ± 1.17	5.80 ± 1.12
2/60	3.92 ± 1.20	1.77 ± 0.15	3.28 ± 0.45	5.06 ± 0.59
2/30	7.10 ± 2.78	2.18 ± 0.11	8.13 ± 1.50	10.31 ± 1.60

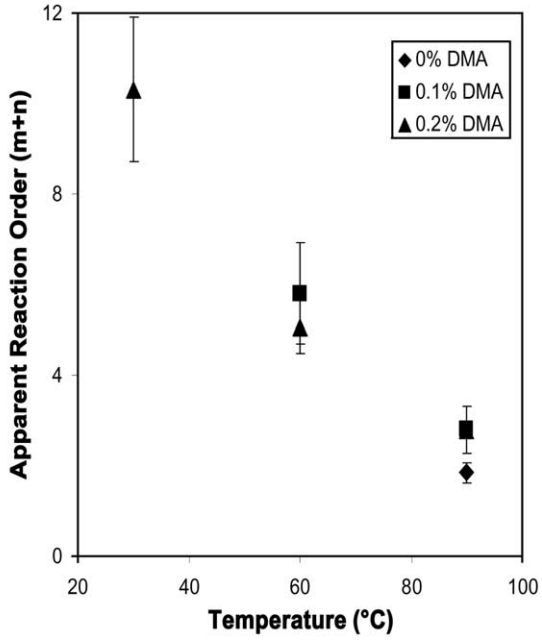

Fig. 11. The apparent reaction order shows a strong temperature dependence.

4. Theoretical understanding of network structure effects on mechanical properties

The tests for the mechanical properties of the VE/S resin show that cure temperature and cure formulation affect the mechanical properties of the resin. Both tensile and fracture properties are maximized and have lower variability when accelerator is not used during the cure. Samples having the poorest mechanical properties were found to have the greatest number of reactions by FTIR, which indicates that accelerated cures at lower temperatures lead to greater cyclization. Through light scattering and SAXS experiments, it became apparent that the differences in mechanical properties are not the result of phase separation. Based on density and swelling experiments, the data indicate that the network structure for these samples is essentially identical and independent of cure schedule or cure formulation. However, such experiments only provide information on the bulk network, indicating that the structural differences are not evident at the bulk scale. Analysis of DSC data indicates modification of cure as a function of both cure temperature and the presence/absence of accelerator.

The previous experiments indicate the significance of initiation conditions in determining the mechanical behavior of the resin. With accelerator, radicals are introduced even at low temperatures where monomer mobility is limited. Therefore, reaction sites are available, but the freedom to react with a random unsaturation is lacking. In such a situation, reactions become localized and intramolecular cross-links are favored over intermolecular cross-links, resulting in the formation of bonds that do not contribute to strength or elasticity of the network. The highest fraction

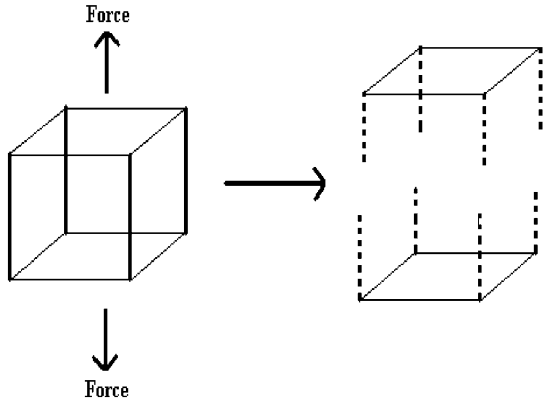

Fig. 12. A perfect elastomeric network cube. The four vertical chains can each bear a load F upon stretching, leading to a maximum tensile strength of $4F$. Once the four vertical chains constituting the lattice break, the system fails.

of loop formation occurs in the beginning of the reaction because of small end-to-end distances that result in limited propagation of radicals away from the newly created pendants. Reactions confined in this manner may lead to highly stressed network configurations.

When reactions occur at high temperatures, system mobility is also high and this generally allows the monomers greater opportunity to achieve a relaxed conformation and minimize stress. With thermal initiation, the introduction of radicals occurs at a slow and steady pace; this, coupled with high mobility, results in the slow process of bulk network formation. However, when accelerated cure occurs at high temperature, the sheer magnitude of radicals released simultaneously results in numerous reactions occurring very rapidly. Upon post-cure, the network structure already formed influences what reactions may or may not be possible during the post-cure; even though monomer mobility is greater at these higher temperatures, many pendant groups may be 'trapped' within highly cross-linked regimes and only allowed to react with neighbors. Hence, when DMA is used for cure, a majority of the reactions is lost to cyclization during the cure, and this continues to affect network formation during post-cure.

This set of behavior can be summarized as follows: (1) temperature determines the mobility of the system; (2) the DMA/BPO pair determines the radical concentration in the system; and (3) radical concentration and molecular mobility work together to define the network structure. Both high mobility and a sufficient radical concentration are required for the creation of a strong network. When radicals are present but mobility is lacking, as in the case of high DMA concentrations at low temperature cures, it is hypothesized that the properties are poor due to extensive intramolecular cross-linking. With fewer intermolecular bonds in the resin, fewer chains are able to bear the load placed on the material, which therefore weakens the mechanical properties of the resin. Such behavior has been theorized in numerous systems.

In epoxy systems, the distribution in network segmental extensibilities controls failure initiation and propagation of the network [26]. The segments with the lowest extensibilities at any given time in the failure process will carry a significant portion of the load and will undergo chain scission resulting in a process of progressive scission of the least extensible segments. Bueche [67] formally developed a theory for elastomeric networks to explain the mechanical behavior of the elastomers. Considering an imaginary, perfect rubber network, Bueche pictured a cube, as shown in Fig. 12, where each network chain was of molecular weight M_c. Upon stretching such a simplified rubber, the entire load must be held by the vertical chains, shown in bold. If there are n vertical strands in the sample of unit original cross-sectional area, and if each chain can hold a load F, the sample will be capable of having a tensile strength of nF. Bersted [68] and Turner [69] presented similar models to account for the large variations in tensile strength and tensile impact strength of amorphous, linear polymers from a consideration of an idealized entanglement network. They also hypothesized that the strength of a material is related to the number of supporting strands or interconnections in the entanglement network.

A similar reasoning, modified to account for the micro-gel behavior, can be applied to the VE/S system studied here. If the corners of the cubic lattice are assumed radical initiation sites, then with low temperature cure employing DMA, each reaction site may be associated with a micro-gel. Most of the reactions will be confined locally to the micro-gels with few cross-links developing to interconnect the micro-gels, as shown in Fig. 13(a). In such a case, if a vertical tensile stress is applied to the cube, then despite the large number of covalent bonds that are present, only four chains will be responsible for bearing the load. Once these four chains have broken, the sample will fail.

However, thermally initiated samples will form a different network structure. Because of the higher mobility of the radical species and the slower release of radicals, far fewer will remain at the site of origination. Rather, many will propagate through the medium and form more of the longer, intermolecular bonds, yielding a structure shown in Fig. 13(b). If a vertical tensile stress is applied to the cube, more chains are able to support the load. Hence, tensile strength is greater than $4F$. As drawn in Fig. 13(b), tensile strength equals $7F$. However, despite the large number of covalent bonds that are present, not all will be responsible for bearing the initial load.

The greater n value explains the greater tensile strength but not the greater ductility of the thermally initiated resins. When the accelerated sample is subject to tensile stress, the load is shared by four vertical chains. Once these four chains break, the sample has failed. When the thermally initiated sample is subjected to tensile stress, only seven chains may share the load at a given time, but as the seven chains break, their share of the load is taken up by another set of chains, and this process continues until the sample fails. This results

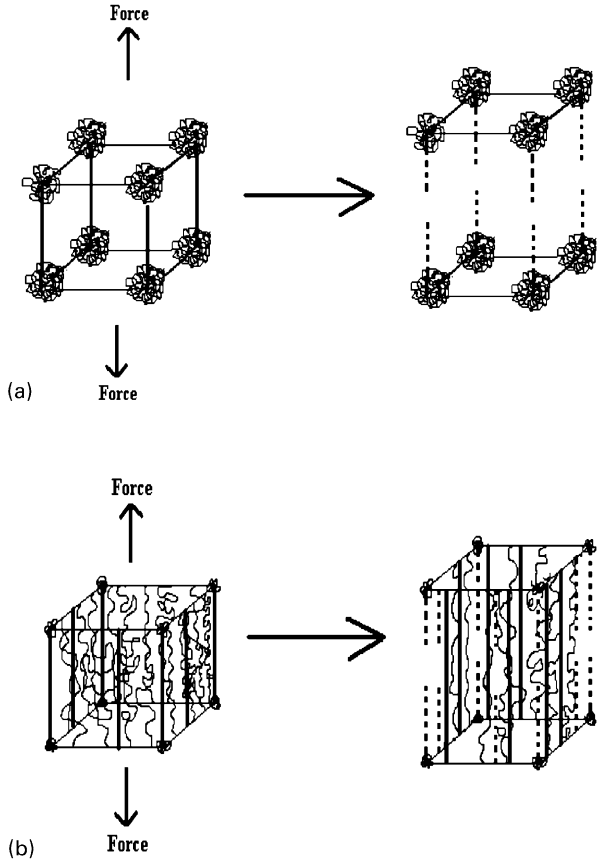

Fig. 13. (a) A hypothetical cubic lattice that may develop for the accelerated VE/S resin as a result of high levels of micro-gel formation. The micro-gels form at the site of radical origination with few intermolecular cross-links to connect them. Despite the large number of covalent bonds in this system, the tensile strength remains at $4F$. The system fails once the four intermolecularly bonded chains break. (b) A hypothetical cubic lattice that may develop for the thermally initiated VE/S resin. A more homogeneous structure is formed allowing for greater strength and ductility. Solid, bold lines represent chains bearing the load; dashed, bold lines represent broken chains; and thin curved lines represent longer chains not yet subject to the load.

in the thermally initiated resin displaying greater ductility. Thus, the thermally initiated network has greater intermolecular bonding that allows for improved mechanical properties, and the accelerated network has greater intramolecular bonding that does not contribute to mechanical strength.

The models developed are also in accord with the free volume explanation for mechanical behavior and the entropy explanation for glass transition trends. The thermally initiated resin minimized rotational restrictions for the chains, allowing for greater free volume and thereby greater strength and mobility. The larger micro-gels of the accelerated resins are highly stressed regions that are unable to accommodate chain movement when a load is applied.

This theory is supported by evidence available for epoxy networks. Morgan [26] investigated the basic ring structures of the network by molecular models to describe the network topography for epoxies. These studies identified sterically feasible ring structures and found that the ability to undergo cooperative deformation is controlled by the regularity of the network topography, determined by the different geometries of the basic rings and their orientation relative to one another. Irregular networks that consist of rings with a variety of geometries develop overstrained segments at lower extensibilities and therefore have lower ultimate network properties. Hence, deformation and failure in epoxies is related to network extensibility that, in turn, is determined by degree of heterogeneity. However, free-radical polymerization has proven to be more heterogeneous than step polymerization; therefore, if heterogeneity can impact physical properties in epoxy systems, the effect is compounded and may take on greater significance in vinyl–divinyl systems. In such a case, the distribution in network segmental extensibilities that controls failure initiation and propagation of the network is even more skewed. This is the essence of the micro-gel.

4.1. Discrepancies in the literature: impact of initiation mechanism

One of the most significant conclusions reached as a result of this research is that the initiation mechanism is important in determining the mechanical properties of the resin. This may explain the reason for contradictory results often observed in the literature. For example, Ziaee and Palmese [1] studied the DERAKANE® 411-C50 resin and found that fracture toughness of samples cured at 30 °C and then post-cured at 125 °C were three times greater than for samples cured at 90 °C and post-cured at 125 °C. In this research, the samples cured at 90 °C had higher fracture toughness values. Stone et al. [70] analyzed the cure kinetics of DERAKANE® 411-C50 at 20–40 °C using a linear regression technique with the assumption that $m + n = 2$. Their results showed good fit with the autocatalytic equation.

The reason for this discrepancy could be related to the type of initiating mechanism. Both researchers used Triginox® 239 A (a mixture of cumyl hydroperoxide, proprietary carboxylic ester, and 2-phenyl isopropanol) as initiator and cobalt naphthenate as promoter. This initiator–promoter system is vastly different from the BPO/DMA system used in this research. First, the Triganox® initiator does not dissociate readily. The cobalt promoter had to be used even at high cure temperatures of 90 °C because the Triganox® showed an induction time of over an hour at this temperature. This is clearly not the case with the BPO initiator which achieves almost complete reaction at cures of 90 °C.

A frequently used initiator system for the cure of UPE/S and VE/S resins is methyl ethyl ketone peroxide (MEKP) with styrene-soluble, multivalent metal salt accelerators such as cobalt naphthenate or octoate. Dissociation of the MEKP into free radicals at ambient temperatures involves a

redox reaction. Although the metal-salt derivatives are effective with organic hydroperoxides such as MEKP, they are ineffective with diperoxides such as BPO [71]. In addition, the reaction can be enhanced by tertiary aromatic amines such as DMA, which appear to be more effective in promoting the transition of the cobalt from the higher to lower valency state [71]. Thus, the driving forces for radical creation in systems involving metal-salt accelerators are different from those encountered in the BPO/DMA initiating system. This research has shown that the network architecture formed during cure is very sensitive to the concentration of radicals released in the resin, their rate of release, and their mobility. The first two factors are determined by the initiating system and the third by cure temperature. Thus, even if cure schedules are identical, a resin may have vastly different properties depending on the mechanism of initiation.

5. Conclusions

An improved understanding of the relationship between cure mechanism, network architecture, and mechanical properties of a free-radical polymerizing thermoset, in this case a VE/S resin system, was achieved. Experiments were performed that examined the mechanical behavior, phase separation behavior, and network structure of the resin as functions of cure schedules and formulation. It was found that using accelerator during cure lowers the tensile strength, strain-at-break, fracture toughness, and strain-energy release rate values and increases the variability of the results. Although the average bulk network properties of all resin formulation/schedule systems studied here are essentially the same, the microscopic network properties are vastly different and account for the differences in mechanical properties. In essence, the release of too many radicals at once into the resin leads to localized reactions, even at higher temperatures. The essential difference between the initiation mechanisms is the difference between bulk reaction (thermal initiation at high cure temperatures) and local reaction (accelerated initiation).

Trends in the autocatalytic equation parameters reveal differences in reaction kinetics that correlate with the observed mechanical properties. Based on the hypothesis developed, the reaction kinetics is able to account qualitatively for resin heterogeneity through the presence of the micro-gels. Thus, one may conclude that while micro-gels form in the vinyl–divinyl system, the extent of micro-gel formation differs dramatically between accelerated and thermally initiated resins. Greater micro-gel concentrations reveal greater heterogeneity in the resin. These results make obvious the fact that the combined effects of DMA concentration and cure temperature determine the network structure and resin properties. At higher accelerator concentration, the reduction in chain mobility is not directly compensated by an increased level of free radicals in the system. Although increasing the cure temperature and increasing radical concentration both lead to a faster reaction, the effect on network structure is not the same.

References

[1] Ziaee S, Palmese GR. J Polym Sci, Polym Phys 1999;37:725.
[2] Yang YS, Lee JL. Polymer 1988;29:1793.
[3] Kloosterboer JG, van de Hei GMM, Boots HMJ. Polym Commun 1984;25:354.
[4] Malinsky J, Klaban J, Dusek K. J Macromol Sci Chem 1971;A5:1071.
[5] Chen JS, Yu TL. J Appl Polym Sci 1998;69:871.
[6] Mortaigne B, Feltz B, Laurens P. J Appl Polym Sci 1997;66:1703.
[7] Brill RP, Palmese GR. J Appl Polym Sci 2000;76:1572.
[8] Naghash HJ, Okay O. J Appl Polym Sci 1996;60:971.
[9] Elliott JE, Bowman CN. Macromolecules 1999;32:6552.
[10] Hsu CP, Lee LJ. Polymer 1993;34:4506.
[11] Lucas JC, Borrajo J, Williams RJJ. Polymer 1993;34:3216.
[12] Ramis X, Salla JM. J Polym Sci, Polym Phys 1999;B37:751.
[13] Hsu CP, Lee LJ. Polymer 1993;34:4496.
[14] Li L, Sun X, Lee LJ. Polym Engng Sci 1999;39:646.
[15] Ganem M, Mortaigne B, Bellinger V, Verdu J. J Macromol Sci, Pure Appl Chem 1993;A30:829.
[16] Chen W, Kobayashi S, Inoue T, Ohnaga T, Ougizawa T. Polymer 1994;35:4015.
[17] Inoue T. Prog Polym Sci 1995;20:119.
[18] Okada M, Fujimoto K, Nose T. Macromolecules 1995;28:1795.
[19] Okada M, Sakaguchi T. Macromolecules 1999;32:4154.
[20] Verchere D, Sautereau H, Pascault JP, Moschiar M, Riccardi CC, Williams RJJ. J Appl Polym Sci 1990;41:467.
[21] Yamanaka K, Inoue T. J Mater Sci 1990;25:241.
[22] Zhang J, Zhang H, Yang Y. J Appl Polym Sci 1999;72:59.
[23] Girard-Reydet E, Sautereau H, Pascault JP, Keates P, Navard P, Thollet G, Vigier G. Polymer 1998;39:2269.
[24] Yang Y, Fujiwara H, Chiba T, Inoue T. Polymer 1998;39:2745.
[25] Elicabe GE, Larrondo HA, Williams RJJ. Macromolecules 1997; 30:6550.
[26] Morgan RJ. Adv Polym Sci 1985;72:1.
[27] Boots HMJ. Physica A 1987;147:90.
[28] Ganem M, Lafontaine E, Mortaigne B, Bellenger V, Verdu J. J Macromol Sci Phys 1994;B33:155.
[29] Varma IK, Rao BS, Choudhary MS, Choudhary V, Varma DS. Angew Makromol Chem 1985;130:191.
[30] Sun B, Yu TL. J Appl Polym Sci 1995;57:7.
[31] Naghash HJ, Okay O, Yagci Y. Polym Bull 1996;37:207.
[32] Chiu YY, Lee LJ. J Polym Sci, Polym Chem 1995;A33:257.
[33] Han CD, Lem K-W. J Appl Polym Sci 1983;28:3155.
[34] Han CD, Lem K-W. J Appl Polym Sci 1984;29:1879.
[35] Lange J, Ekelof R, George GA. Polymer 1999;40:3595.
[36] Jacobs PM, Jones FR. Polymer 1992;33:1418.
[37] Pryor WA, Hendrickson Jr WH. Tetrahedron Lett 1983;24:1459.
[38] Yildiz U, Hazer B. Polymer 2000;41:539.
[39] Moreau M, Chappard D, Lesourd M, Montheard JP, Basle MF. J Biomed Mater Res 1998;40:124.
[40] Wolf AV, Brown MG, Prentiss PG. Handbook of chemistry and physics. 67th ed. Boca Raton: CRC Press. p. D-254.
[41] Kausch H-H. Polymer fracture. New York: Springer, 1986.
[42] Martin JL. Polymer 1999;40:3451.
[43] Lem K-W, Han CD. Polym Engng Sci 1984;24:175.
[44] Cook WD, Simon GP, Burchill PJ, Lau M, Fitch TJ. J Appl Polym Sci 1997;64:769.
[45] Huang Y-J, Chaur-Jeng C. J Appl Polym Sci 1992;48:1573.
[46] Huang Y-J, Su C-C. J Appl Polym Sci 1995;55:305.
[47] Nielsen LE. Mechanical properties of polymers and composites, vol. 2. New York: Marcel Dekker, 1974.

[48] Roe RJ. Encyclopedia of polymer science and engineering, vol. 7. New York: Wiley-Interscience, 1987. p. 539.
[49] Martin JS, Laza JM, Morras ML, Rodrigues M, Leon LM. Polymer 2000;41:4203.
[50] Gaur B, Rai JSP. Eur Polym J 1993;29:1149.
[51] Gonzalez-Romero VM, Cassillas N. Polym Engng Sci 1989;29:295.
[52] O'Neil GA, Torkelson JM. Macromolecules 1999;32:411.
[53] O'Neil GA, Wisnudel MB, Torkelson JM. Macromolecules 1998; 31:4537.
[54] O'Neil GA, Torkelson JM. Trends Polym Sci 1997;5:349.
[55] O'Neil GA, Wisnudel MB, Torkelson JM. Macromolecules 1996; 29:6193.
[56] Kamal MR, Sourour S. Polym Engng Sci 1973;13:59.
[57] Atarsia A, Boukhili R. Polym Engng Sci 2000;40:607.
[58] Moroni A, Mijovic J, Pearce EM, Foun CC. J Appl Polym Sci 1986;32:3761.
[59] Kenny JM. J Appl Polym Sci 1994;51:761.
[60] Chung T-S. J Appl Polym Sci 1984;29:4403.
[61] Keenan MR. J Appl Polym Sci 1987;33:1725.
[62] Ryan ME, Dutta A. Polymer 1979;20:203.
[63] Lee JH, Lee JW. Polym Engng Sci 1994;34:742.
[64] Pusatcioglu SY, Fricke AL, Hassler JC. J Appl Polym Sci 1979; 24:937.
[65] Sourour S, Kamal MR. Thermochim Acta 1976;14:41.
[66] Wen M, McCormick AV. Macromolecules 2000;33:9247.
[67] Bueche F. Rubber Chem Technol 1959;32:1269.
[68] Bersted BH. J Appl Polym Sci 1979;24:37.
[69] Turner DT. Polymer 1982;23:626.
[70] Stone MA, Fink BK, Bogetti TA, Gillespei Jr JW. Polym Engng Sci 2000;40(12):2489.
[71] Selly J. Encyclopedia of polymer science and engineering, vol. 12. New York: Wiley-Interscience, 1988. p. 269.